



A chemical interpretation for the post-reversion upturn in the natural rubber/accelerated sulfur system based on the viscoelastic properties and cross-link density measurements

Marek Pöschl¹ · Shibulal Gopi Sathi¹ · Radek Stoček¹

Received: 30 December 2023 / Revised: 21 March 2024 / Accepted: 29 April 2024
© The Author(s) 2024

Abstract

The curing cycle of natural rubber (NR) with a conventional accelerated sulfur system (CV) generally exhibits three phases. The induction phase, the crosslinking phase, and the reversion phase. Prolonged curing of NR/CV system even at a temperature of 150 °C can show reversion. Many research reports are available in the literature with reference to the reversion behavior and the subsequent network modifications of natural rubber with accelerated sulfur. However, the literature regarding post-reversion curing behavior is scanty. This article describes the post-reversion upturn of natural rubber with a conventional accelerator sulfur system at a higher curing temperature. A network rebuilding after collapsing the initially formed network due to reversion was identified as the primary reason for the post-reversion upturn. The dynamic rheological testing capability of the Rubber Process Analyzer (RPA) was employed to characterize the network formed during curing, reversion and post-reversion phases. The cure-strain sweep data from the RPA indicated that the shear storage modulus (G') of the broken network increased due to the post-reversion upturn. The chemical crosslink densities of the samples were also found to increase due to the upturn curing behavior. From these experimental results and the information conceived from the previous literature, two plausible mechanisms have been proposed to interpret the post-reversion upturn cure behavior.

Keywords Natural rubber · Post-reversion · Rubber process analyser · Strain sweep · Storage modulus

✉ Shibulal Gopi Sathi
gslal2009@gmail.com

¹ Centre of Polymer Systems, Tomas Bata University in Zlín, Třída Tomáše Bati 5678, 760 01 Zlín, Czech Republic

Introduction

The last and most crucial step in the production of any rubber product is curing, often known as vulcanization. During curing, the rubber chains connected each other by chemical bonds, forming a three-dimensional network structure. The rubber products attain the required strength, dimensional stability, and elastic recovery only after the curing process. Because of its unsaturated backbone with active allylic carbon atoms, NR is often cured with a combination of elemental sulfur (S_8), activators (typically zinc oxide/stearic acid combinations), and appropriate accelerators to expedite the curing process. Rubber chains are connected by sulfur atoms during the accelerated sulfur curing of NR. The accelerator-to-sulfur ratio determines which combinations of poly-sulfidic, di-sulfidic, and mono-sulfidic are typically involved in these linkages. It is well known that a conventional vulcanization (CV) system possesses the highest amount of sulfur (usually in the range of 2–3.5 phr) and the lowest amount of accelerator (1.2–0.4 phr). Therefore, the accelerator-to-sulfur ratio of a CV system lies in between 0.1 to 0.6. Since the sulfur level is high in a CV system, the curing of NR with a CV system results a vulcanizate with 95% poly and di-sulfidic crosslinks and 5% of mono-sulfidic crosslinks. If the sulfur level is maintained in the range of 1.0–1.7 phr and the accelerator level is in the range of 2.5–1.2 phr, this constitutes a semi-efficient vulcanization (SEV) system with an accelerator-to-sulfur ratio in the range of 0.7–2.5. The curing of NR with a SEV system results in a vulcanizate with 50% poly and di-sulfidic crosslinks and 50% mono-sulfidic crosslinks. For vulcanizates with high amounts of mono-sulfidic crosslinks, it is recommended to use an efficient vulcanization (EV) system. For an EV system, the recommended sulfur level is 0.4–0.8 phr, and the accelerator level is 5.0–2.0 phr. Therefore, the accelerator-to-sulfur ratio of an EV system is in the range of 2.5–12.5. Generally, the vulcanizate of NR with an EV system comprises 80% mono-sulfidic, and the rest 20% constitutes poly- and di-sulfidic crosslinks. Among the three types of accelerated sulfur systems, the vulcanizate of NR with a CV system offers high flex-fatigue resistance and tear resistance. However, because of the low bond dissociation energy (252 kJ/mol) of the poly-sulfidic crosslinks, the NR/CV system exhibits low heat aging resistance and poor reversion (network disruption due to over curing) resistance [1–5].

Curemeters such as the moving die rheometer (MDR) and the rubber process analyzer (RPA) are widely employed to investigate the curing behavior and the reversion characteristics of rubbers. The curemeter consists of two biconical dies that are capable of oscillating to a predetermined strain and frequency at the required test temperature. As the compounded rubber that is placed between the preheated biconical dies of the rheometer vulcanizes, the torque required to maintain the pre-fixed oscillatory deformation of the lower die increases as a function of time. The torque registered as a function of time obtained from the rheometer is called the rheogram or the curing profile of a rubber compound [6, 7]. A typical curing curve of a NR with a CV system starts with an induction period where no crosslinking is taking place. However, crosslink precursors such as sulfurating species will be created at this stage. Flowing and forming of the rubber compound within the mold cavity will

also take place during the induction period. After the induction period, the rubber chains get connected to each other via sulfur linkages and form a network structure with a majority of poly-sulfidic crosslinks. As a result, the torque due to crosslinking continues to increase and then reaches its maximum value (maximum torque, S'_{max}). If the temperature of curing is set at 130 °C, the cure curve exhibits a plateau region immediately after the S'_{max} , where torque will be independent of time. However, if the cure temperature of the NR/CV system is above 150 °C, the cure curve exhibits a sharp declination immediately from the point of S'_{max} due to reversion. Many reports are available in the literature concerning the reversion of natural rubber and other synthetic elastomers during curing with the accelerated sulfur system [8–11]. One of the widely accepted reasons for the modulus drop due to reversion is the desulfuration of the initially generated poly-sulfidic crosslinks and their rearrangements into more thermally stable di- and mono-sulfidic crosslinks.

In the present investigation, the curing profiles of NR/CV system generated from MDR at different temperatures were carefully examined. Interestingly, it has been noticed that the curing curves exhibit an upturn behavior after a strong reversion at a temperature from 180 °C and above. To further scrutinize the network modifications in the cured sample, the viscoelastic testing capabilities of RPA have been utilized. Unlike MDR, the lower die of the RPA can apply sinusoidal shear deformation to the cured sample under different strains and frequency ranges. The modern RPA (Premier RPA) by Alpha Technologies offers a temperature range from ambient to 230 °C, a strain range of 0.07 to 1255% and a frequency of oscillation of 0.001 to 50 Hz. Moreover, the latest Alpha's sub-zero technology claims that it is possible to cool the RPA dies down to -25 °C without the use of liquid nitrogen. This allows us to perform the viscoelastic studies in shear mode under a wide temperature range from -25 to 230 °C. By applying appropriate strain and frequency combinations at a predetermined test temperature, the viscoelastic parameters (storage modulus (G'), loss modulus (G''), and $\tan \delta$ (G''/G')) of the cured sample can be evaluated. In this study, the cure-strain sweep measurement capability of RPA has been utilized to evaluate the network strength (G') resulting from the post-reversion upturn. To the best of our knowledge, this is the first report in the literature dealing with the post-reversion upturn in the NR/CV system, along with a chemical interpretation based on the RPA test results and the crosslink density measurements.

Experimental

Materials

The natural rubber used in this study was a constant viscosity standard Vietnamese rubber with a Mooney viscosity ML(1+4) at 100 °C: 60 ± 5 obtained from Binh Phuoc, Vietnam, under the trade name SVR CV60. 1, 3- bis(citraconimidomethyl) benzene (Perkalink 900; PL) was used as the dieneophile. This chemical was obtained from Lanxess Deutschland GmbH, Leverkusen, Germany. All other ingredients such as dicumyl peroxide (DCP), sulfur; n-cyclohexyl-2-benzothiazole

sulfenamide (CBS); stearic acid, and zinc oxide were purchased from Sigma-Aldrich, Czech Republic.

Preparation of rubber compounds

The rubber compounds were prepared as per the formulations and are displayed in Table 1. All the compounds were prepared using a 0.4-L Farrel Pomini mini lab Banbury mixer (GmbH & Co. KG, Germany). A fill-factor of 0.75 was taken for the efficient mixing of the ingredients. The NR was masticated for one minute at 50 °C and 60 rpm. To this, the ZnO and stearic acid were added, and the mixing was continued for up to 5 min. The mix is then taken out of the Banbury mixer and homogenized for one minute using a two-roll mill. The homogenized batch is again taken back into the Banbury mixer, where the curatives (sulfur, CBS, and PL) were added and mixed for 3 min at 50 °C under 60 rpm. After the mixing, the whole mix was discharged and again homogenized using a two-roll mill for 5 min to get a better dispersion of the curatives into the rubber matrix. The mix was then molded into sheets with a thickness of 2 mm using a compression molding heat press LaBEcon 300 (Fontijne Presses, The Netherlands) for different curing according to the rheometer cure data and nature of the curing curves.

Characterization

Cure characteristics

A moving die rheometer (MDR-3000, Mon Tech, Germany) as per ASTM D 5289 was used to measure the curing parameters such as maximum torque: S'_{max} , minimum torque: S'_{min} , the difference between maximum and minimum torque: $\Delta S'$ (This can be considered as an indirect measure of the crosslink density), scorch time: T_{S2} (This indicates the mold filling time or flow time of the rubber compound without any pre-mature vulcanization). Optimum cure time: T_{90} (the time required for the torque to reach 90% of the maximum torque).

Cure-strain sweep test

As mentioned in the introduction, this test was designed to understand the strength of the network formed during the post-reversion phase in terms of the shear storage modulus (G') as a function of amplitude sweep. For this, a new

Table 1 Formulation of the mixes

Sample ID	Ingredients						
	NR	ZnO	Stearic acid	Sulfur	CBS	DCP	PL
NR-S	100	4	1	2	0.5	–	–
NR-SPL1	100	4	1	2	0.5	–	1
NR-D1	100	–	–	–	–	1	–

testing program has been created as shown in Fig. 1 using a Premier Rubber Process Analyzer (RPA) from Alpha Technologies, USA. As per this program, the test sample was first allowed to cure at 180 °C up to the pre-fixed curing time. The test samples' corresponding curing curves, which were already generated for an hour at 180 °C, were used to pre-fix the curing time. The cured sample is then allowed to cool down to 40 °C within the RPA die, and a strain sweep was immediately performed from 0.05 to 100% at a frequency of 1 Hz to measure the G' .

Chemical crosslink density

The equilibrium swelling method using toluene was used to calculate the crosslink density of the samples molded at different temperature for different time. The cured samples of dimensions 20×30×2 mm were allowed to swell in toluene until they achieved the equilibrium swelling state. Taken out the swollen samples and weighed immediately after removing the solvent retained on the surface of the samples using blotting paper. Then, the swollen samples were dried and weighed again to calculate the volume fraction of rubber using the Eq. (1). By substituting the values of V_r in Eq. (2) developed by Flory and Rehner, the chemical crosslink densities (n) of the samples were calculated [12, 13].

$$V_r = \frac{W_d}{W_d + (W_s - W_d) \frac{\rho_r}{\rho_s}} \tag{1}$$

$$n = \frac{[\ln(1 - V_r) + V_r + \chi V_r^2]}{V_s \left[V_r^{1/3} - \frac{V_r}{2} \right]} \tag{2}$$

W_s is the swollen weight of the sample, W_d is the dried weight, ρ_r is the density of the rubber, ρ_s is the density of the solvent, V_r is the volume fraction of rubber in the equilibrium swollen sample, V_s is the molar volume of the solvent (106.3 mL/mol for toluene at room temperature) and χ is the Flory–Huggins interaction parameter. For NR-toluene system, the value of χ was taken as 0.414 [14].

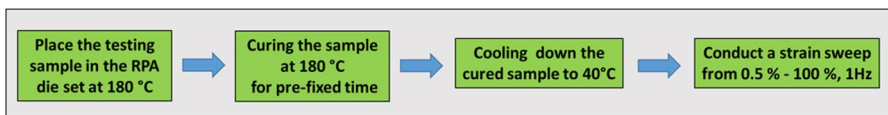


Fig. 1 Testing protocol for the cure-strain sweep analysis

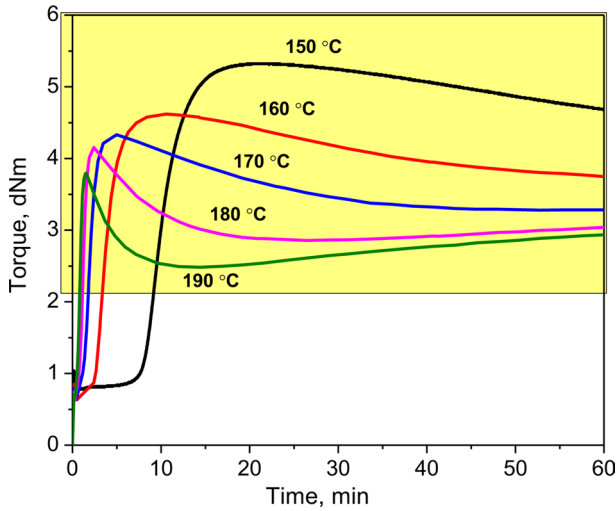


Fig. 2 Curing curves of NR-S at different temperatures for 1 h

Table 2 Curing characteristics of the mixes

Sample ID	Tempt. (°C)	Curing parameters					
		S'_{\min} (dNm)	S'_{\max} (dNm)	$\Delta \Sigma \ni (\delta N\mu)$ ($S'_{\max} - S'_{\min}$)	T_{S_2} (min)	T_{90} (min)	CRI (min^{-1}) ($100/T_{90} - T_{S_2}$)
NR-S	150	0.78	5.32	4.54	9.73	3.56	26.17
	160	0.64	4.62	3.98	3.08	8.38	37.59
	170	0.63	4.36	3.73	1.59	1.99	77.51
	180	0.64	4.15	3.51	1.01	5.04	192.3
	190	0.66	3.8	3.14	0.72	1.01	344.82
NR-SPL1	180	0.65	4.94	4.29	1.45	37.71	2.75
NR-D1	180	0.68	3.65	2.97	0.73	2.83	47.61

Results and discussion

Curing analysis of NR-S at different temperatures

Represented in Fig. 2 are the curing curves of NR-S at different temperatures from 150 to 190 °C for a fixed time of 1 h. The cure data depicted in Table 2 reveals that the extent of curing ($\Delta S'$) is the highest (4.54 dNm) at 150 °C. The $\Delta S'$ gradually decreased as the time and temperature of curing increased. For instance, the $\Delta S'$ of the network produced at 180 °C was 22.7% lower than the $\Delta S'$ of the network produced at 150 °C. As the temperature rose to 190 °C, the $\Delta S'$ was further reduced to 30.8% compared to the $\Delta S'$ of the 150 °C cured sample. This indicates that the number of poly-sulfidic crosslinks in the fully-grown network decreases as the

curing temperature of the sample increases. This may be one of the probable reasons for the gradual reduction in $\Delta S'$ with increasing the curing temperature. While extending the curing time even after the curing curve reaches its maximum torque (after developing the full-grown network structure), a severe declination in the cure curve was observed. One of the widely accepted reasons for this is considered to be the desulfuration and disruption of the initially formed poly-sulfidic crosslinked network into shorter forms of di- and mono-sulfidic crosslinked network, commonly known as reversion. To understand more about the nature of reversion, the curing curves of the highlighted segment of Fig. 2 is individually displayed in Fig. 3a-e. As can be seen that at 150 °C, the onset of reversion start at 21.5 min followed by a sharp declination till 60 min. The onset of reversion shifted to 10.5 min as the curing temperature increased to 160 °C. From there, a gradual reduction in the curing torque was noticed till the end of the given curing time. At 170 °C, after a declination from 5.0 to 40 min, the curve exhibited a plateau region. Interestingly, at 180 °C, after a sharp declination from 2.5 to 26 min, the curve shows an upturn behavior like a hockey stick (as shown in the inset of Fig. 3d) till 60 min of curing. More or less similar trend was also noticed at 190 °C. However, here it is worth noting that the reversion regime was significantly confined between 1.5 to 13 min. Afterward, the curve exhibited an upturn behavior till 60 min as seen in Fig. 3e.

Influence of curing time and temperature on the reversion behavior of NR-S

The intensity of reversion at different time intervals has been evaluated using Eq. (3) [15, 16]

$$\text{Reversion (\%)} = \frac{S'_{\max} - S'_{\max+t}}{S'_{\max}} \times 100 \quad (3)$$

The percentage reversion calculated after 10 min of curing ($S'_{\max+10 \text{ min}}$) from the maximum torque (S'_{\max}) and after different intervals of time from the beginning of curing at different temperatures are reported in Fig. 4a and b. The magnitude of reversion exhibits a steady increasing trend with increasing the curing temperature after 10 min of curing from the maximum torque which is clear from Fig. 4a. The high severity of network disruption due to desulfuration of the poly-sulfidic crosslinks at a higher temperature is responsible for the higher reversion. Reversion was also depended on the curing time. From Fig. 4b, it is clear that at a given temperature, the reversion increases as the curing time increases. For instance, no reversion was observed in NR-S up to 15 min of curing at 150 °C. However, the reversion increases to 1.5 and 12.0% as the curing time extended to 30 min and 60 min, respectively. However, this trend was maintained only up to 170 °C. Interestingly, because of the upturn in the cure curve after 26 min of curing at 180 °C, the percentage reversion calculated at 60 min was around 1.2 and 4.3% lower than the reversion measured after 15 and 30 min of curing, respectively. The pattern of reversion that was seen as a function of curing time from 150 to 170 °C was exactly the opposite at 190 °C. That means, the severe network breakdown from the point of S'_{\max} causes a higher reversion (34.8%) up to 15 min of curing at

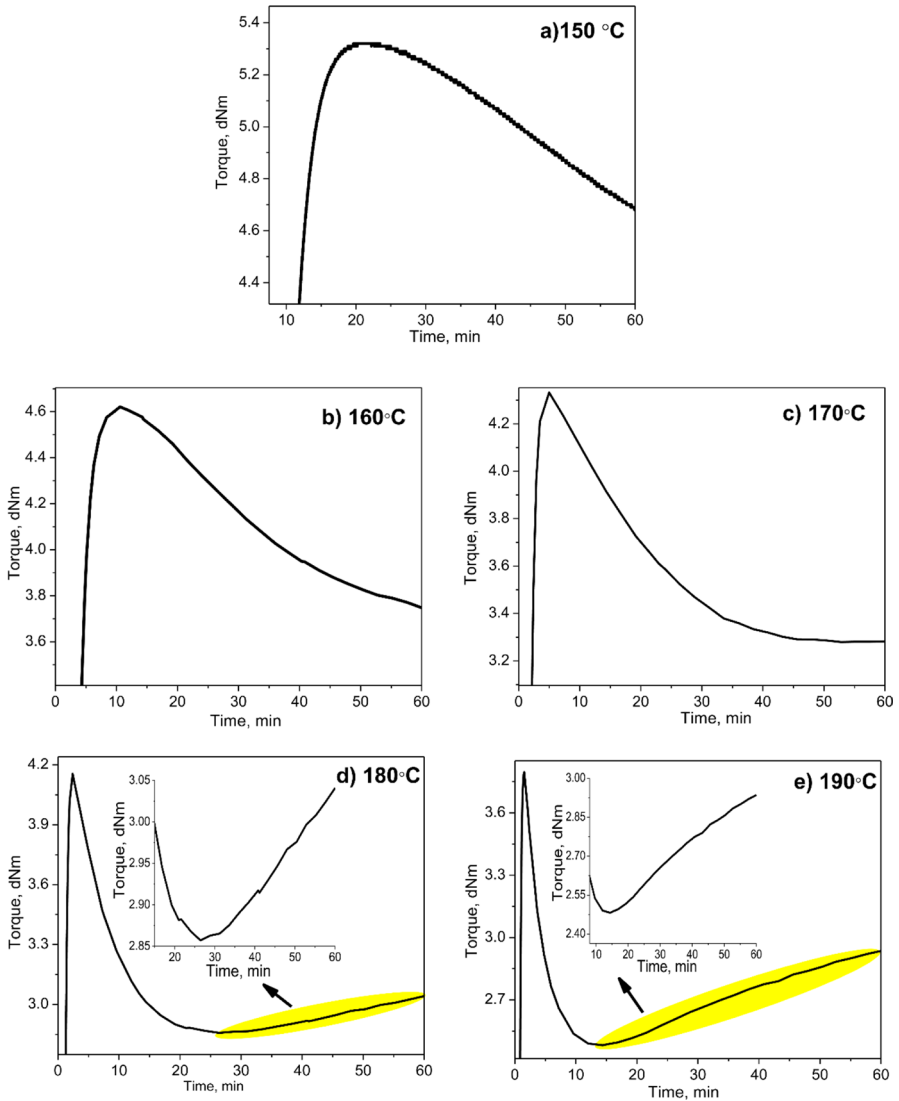


Fig. 3 Curing curves of the highlighted portion of Fig. 1 at different temperatures for 1 h

190 °C. Since there observed a post-reversion cure upturn from 13 to 60 min, the reversion measured at 30 min was 30.4%, which was around 4.4% lower than the reversion exhibited at 15 min. As the curing time extended to 60 min, the reversion was further reduced to around 23.3%. It is important to note that no reports have been previously published in the literature to validate the authenticity of the upturn cure behavior of the NR/CV system after reversion beyond 180 °C. Therefore, to a little more clarity in this aspect, a cure curve of NR with 1 phr DCP (NR-D1) was created at 180 °C for 1 h, as depicted in Fig. 5. It is well known that the curing

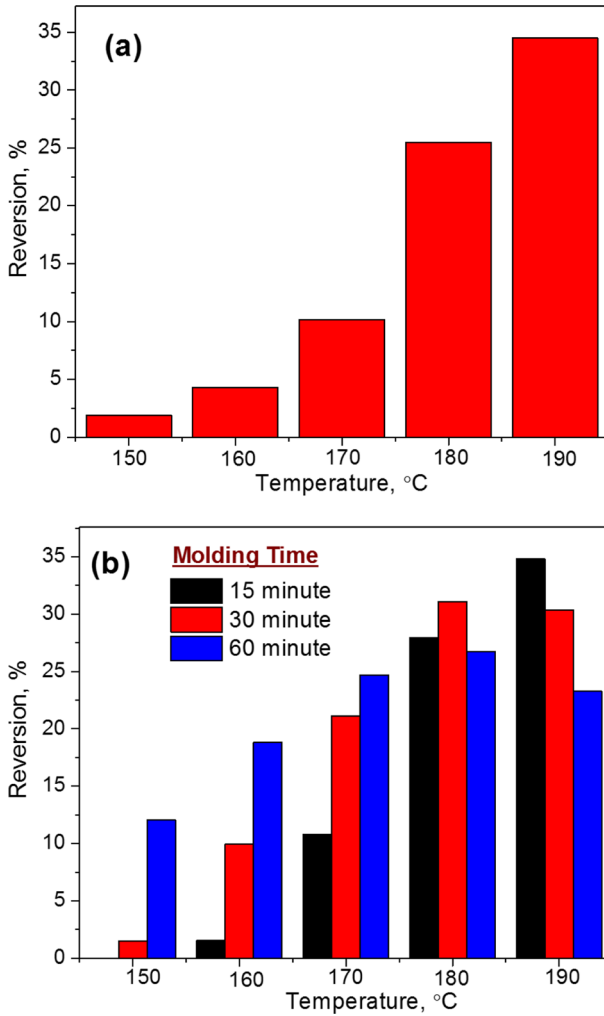


Fig. 4 Percentage reversion of NR-S **a** After 10 min of curing from S'_{max} at different temperatures **b** At different intervals of time from the beginning of curing at different temperatures

of NR with DCP produce carbon–carbon crosslinks between the rubber chains. These crosslinks, because of their high bond dissociation energy (~ 350 kJ/mol), are expected to be thermally very stable even at a high vulcanization temperature [2]. As expected, after attained a maximum torque within 6.7 min of curing, NR-D1 exhibited a perfect plateau region till the end of the given 60 min of curing. This experimental inference confirms that the prolonged curing of NR/CV system at a temperature beyond 180 °C impart certain structural modifications due to desulfuration during the reversion (network break down) phase. These structural modifications may lead to some sort of crosslinking reaction within the broken network. As a result, the strength of the broken network again start to rebuild after

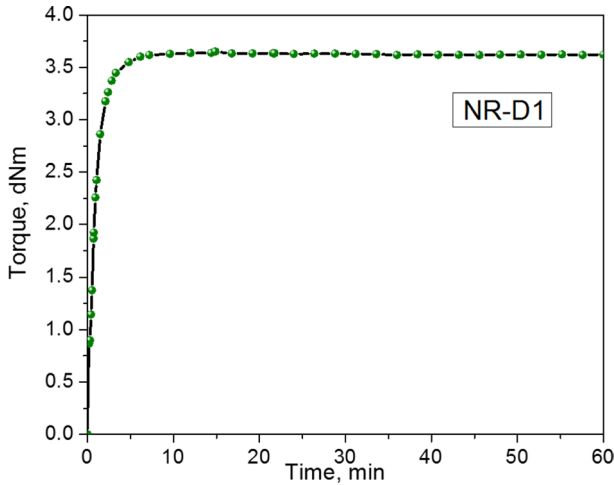


Fig. 5 Curing curve of NR with 1phr DCP at 180 °C, 1 h

the reversion. This network rebuilding is responsible for the cure upturn in NR/CV system after a severe reversion phase during prolonged curing beyond 180 °C.

RPA cure-strain sweep analysis

This test was performed to check the strength of the rebuilt network after the reversion phase. It is well known that the strength and stiffness of the cured network depends on the crosslink density. Higher the crosslink density, higher will be the strength of the cured network. In most of the cases, from the curing curve of a rubber compound, it is possible to conceive some idea about the magnitude of the crosslink density at a particular time. To further validate this, the curing behavior of NR-S at 180 °C was examined for 2 h and the result is depicted in Fig. 6a. This curing curve indicates that the NR-S molded (cured) up to 2.5 min will have the largest crosslink density and, hence, the strongest (modulus). The strength of the 30 min molded NR-S will be the lowest due to the significant disruption of the initially framed network out of poly-sulfidic crosslinks. The strength of a 90-min molded NR-S is anticipated to be in between 2.5 and 30 min molded compounds due to the additional crosslink formation (upturn cure behavior) beyond 30 min of curing. To look over how the curing behavior of NR-S depicted in Fig. 6a will reflect its shear storage modulus (G'), a cure-strain sweep analysis was performed and the results of G' as a function of strain amplitude is displayed in Fig. 6b. The G' curves do not show any perfect pattern with the increase in strain amplitude. However, the magnitude of the G' curves were in good agreement with the torque values of the cure curve at 2.5, 30, and 60 min as shown in Fig. 6a. That means, the strain sweep performed on the 2.5 min cured NR-S exhibited the highest G' over the entire strain range from 0.5–100%. This indicates that the network formed up to 2.5 min of curing was the strongest. Because of the severe network breakdown beyond 2.5 to 30 min of curing, the G' curve of the 30 min cured NR-S was found to be the lowest.

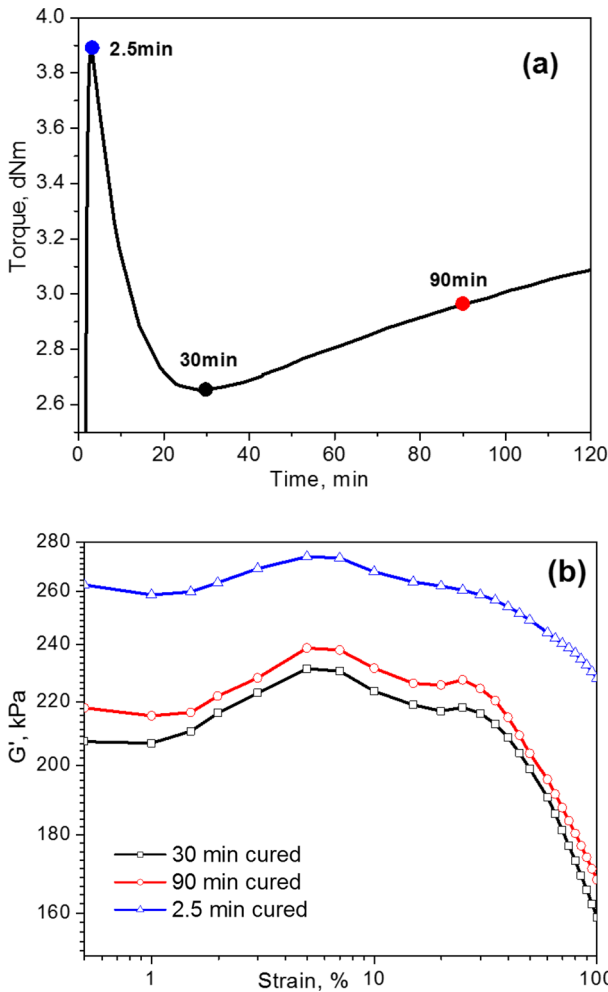


Fig. 6 **a** Curing profile of NR-S at 180 °C, 2 h from MDR **b** Cure-strain sweep curves of NR-S from RPA at 180 °C

The intriguing observation was that the G' curve of the 90-min cured NR-S occupied a position well below and slightly above the G' curves of the 2.5 and 30 min cured NR-S, respectively. This cure-strain sweep results confirms that the strength of the rebuilt network is considerably higher than the network of a 30 min cured compound due to the formation of some new crosslinks after a severe reversion phase.

The crosslink density measurements

The differences in the curing torque at a particular time ($\Delta S'_t$) was calculated from the curing curves shown in Fig. 2 using $\Delta S'_t = S'_t - S'_{min}$; where S'_t is the torque corresponding to the network formed at a time 't', and S'_{min} is the

minimum torque. It is well known that $\Delta S'_t$ can provide an indirect assessment of the crosslink density. However, to further ascertain whether the upturn cure behavior has resulted in the formation of extra crosslinks, the chemical crosslink density of NR-S molded at different temperatures was also measured as a function of molding time using the equilibrium swelling method. Depicted in Fig. 7a, b are the $\Delta S'_t$ vs curing time and the chemical crosslink density *versus* curing time at different curing temperatures, respectively. From Fig. 7a it is

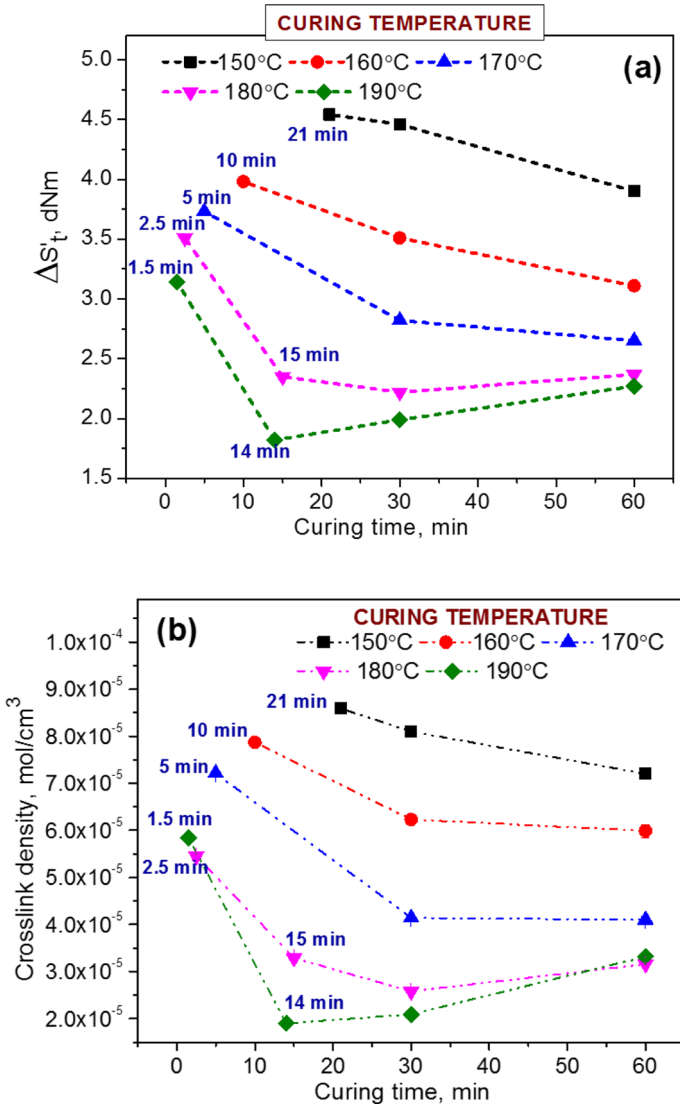


Fig. 7 a $\Delta S'_t$ versus curing time b Chemical crosslink density versus curing time at different curing temperature

clear that, 21 min of curing at 150 °C, NR-S produces a network structure with maximum number of poly-sulfidic crosslinks with a higher network strength, $\Delta S'_t$. As the curing time extended beyond 21 min, the network strength decreases due to the breakage of some initially formed poly-sulfidic crosslinks from the network. When the curing temperature increases to 160 °C, it took only 10 min to achieve a full-grown network structure based on poly-sulfidic crosslinks. Beyond 10 min, the network strength decreases continuously. The time required to create a fully developed network structure drops to 5 min as the curing temperature rises to 170 °C. After five minutes of curing, the network strength gradually decreases. The network grows to full size in 2.5 min of curing at 180 °C; however, it loses 33% of its strength when the curing time increases to 15 min. The loss of network strength between 15 to 30 min of curing was only 5.5%. Here it is worth noting that the broken network gains 6.8% of strength as the curing time extended from 30 to 60 min. The trend was approximately the same as the curing temperature raised to 190 °C too. After attained a full-grown network structure in 1.5 min of curing, a 42% loss of network strength was experienced as the curing time extended to 14 min. Interestingly, the disrupted network gains around 24.7% strength as the curing time increases from 14 to 60 min at 190 °C.

In connection to the variations of $\Delta S'_t$ of NR-S at different temperatures, the crosslink density of NR-S cured at 150 °C for 21 min exhibited the highest value (8.59×10^{-5} mol/cc). It is then gradually decreased by 5.7 and 16.2% as the molding time increased to 30 min and 60 min respectively. At 160 °C, the fully-grown network structure developed within 10 min of curing showed a slightly lower crosslink density (7.87×10^{-5} mol/cc) compared to the fully-grown network developed at 150 °C. The crosslink density then decreased by 20.8 and 23.9% as the curing time increased to 30 and 60 min, respectively. This trend was remains consistent till the curing temperature increases up to 170 °C. However, at 180 °C, the full-grown network formed within 2.5 min of curing exhibited a crosslink density of (5.45×10^{-5} mol/cc). As the curing time extended up to 30 min, around 52.6% crosslink loss has been observed from the network. It was interesting to note that when we increased the curing time from 30 to 60 min, the network formed after 60 min exhibited around 22.5% higher crosslink density than the network formed during the first 30 min of curing. Similarly, with reference to the behavior of $\Delta S'_t$ at 190 °C, the crosslink density of NR-S cured at 190 °C for 1.5 min showed the highest value (5.84×10^{-5} mol/cc), and then sharply declined to 67.5% (1.89×10^{-5} mol/cc) up to 14 min of curing. Around 10% increment in the crosslink density was observed by extending the curing time from 14 to 30 min. As the curing time increased from 30 to 60 min, the crosslink density was further increased by 58.8%. Put another way, by increasing the curing time from 14 to 60 min, approximately 25% of the crosslinks that were lost during the first 14 min of curing at 190 °C could be recovered. The aforementioned details prompted us to understand the potential crosslinking reactions that could lead to the cure upturn of NR-S after a severe reversion phase at curing temperatures 180 °C and above.

Predicted crosslinking mechanisms triggering the post-reversion cure upturn

It has been well documented in the literature that the initial step in the accelerated sulfur curing process is the combination of accelerator and the activator to the formation of active accelerator complex. This accelerator complex then reacts with the elemental sulfur (S_8) to produce several sulfurating species. These sulfurating species reacts with the unsaturated sites (allylic carbon) of the NR chains and attached on to it as accelerator-terminated poly-sulfidic pendant groups known as crosslink precursor. When these crosslink precursors reacts with another unsaturated rubber chains of NR leads to the formation of a poly-sulfidic crosslinks between the two [1, 2, 17, 18]. It has also been reported that prolonged curing of NR with an accelerator sulfur results several modification in the cured network depending upon the accelerator-to-sulfur ratio and the temperature of curing [19–22]. Detailed spectroscopic investigations have proved that these modifications mainly include the conversion of poly-sulfidic crosslinks into mono-, and di-sulfidic crosslinks, cyclic mono- and di-sulfides, unreacted accelerator-terminated crosslink precursor, isomerized double bonds (trans-methine structure). More importantly, the presence of conjugated unsaturated bonds (dienes and trienes) were also been detected on the backbone of some of the NR chains in the cured network [23–25]. Based on these literature information, and also from our cure data, two possibilities have been proposed to justify the upturn cure behavior that we have observed in our system.

(a) *Formation of post-reversion mono-sulfidic crosslinks*

The curing curves of NR-S are demonstrated in Fig. 2 clearly showed that the curve obtained at 150 °C exhibited the highest extent of cure ($\Delta S'$), even though the time to optimum cure (T_{90}) is relatively high. This indicates that at 150 °C, the crosslink precursors that are being formed during the induction period are getting enough time to interact with the maximum number of unsaturated carbon atoms in the rubber chains to form a crosslinked network via poly-sulfidic linkages. Therefore, it is reasonable to believe that the number of unreacted crosslink precursors and unreacted unsaturated backbones may be very few in the fully-grown network structure at 150 °C. As the curing temperature increases, the gelation time decreases. That means, at a higher temperature, the crosslink precursor forms a network structure of poly-sulfidic crosslinks so quickly. As a result, the viscosity of the reactive system increases quickly, which makes it difficult for all the crosslink precursors to find the necessary unsaturated sites in the rubber chains to get crosslinked. This may be one of the reasons why the extent of network formation is shown to be decreasing as the curing temperature increases from 150 to 190 °C. Therefore, it is rational to believe that as the curing temperature of NR-S increases, both the unreacted crosslink precursor and the unreacted NR backbones will be high in number. During the course of the reaction, there is a high possibility for this unreacted crosslink precursor to get trapped within the initially framed network structure as pendant dangling units.

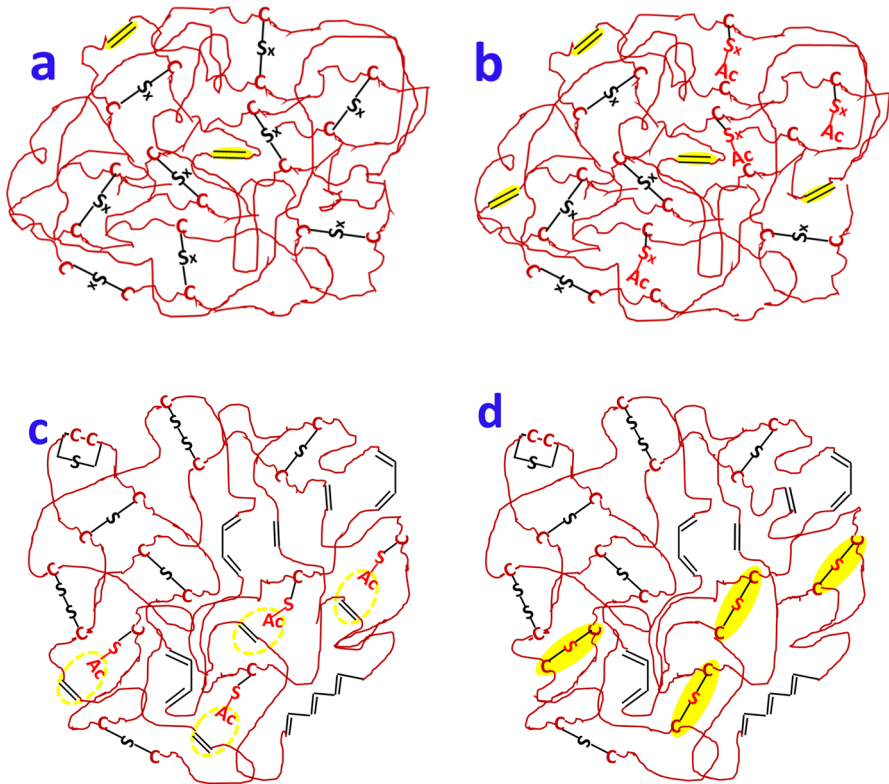


Fig. 8 Presumed network states in NR-S at different temperature and time of curing **a** up to 21 min of curing at 150 °C **b** up to 2.5 min of curing at 180 °C **c** up to 26 min of curing at 180 °C **d** up to 60 min of curing at 180 °C

A pictorial representation of the network being formed just before reversion at 150 °C and at 180 °C (> 180 °C) is depicted in Fig. 8a, b. From Fig. 8a, it is clear that the network mainly consists of uniformly distributed poly-sulfidic crosslinks with no unreacted pendant crosslink precursor. On the other hand, the network formed at 180 °C (or 190 °C) just before reversion consists of a mixture of poly-sulfidic crosslinks as well as some unreacted pendant crosslink precursors. It has been noticed that the intensity of network disruption gradually increases as the curing temperature increases from 150 to 190 °C (Fig. 3). Due to the extreme network disruption that happens over 180 °C (roughly 25% at 180 °C and 34.5% at 190 °C), the overall viscosity of reactive system may marginally decrease after the completion of the reversion phase [26]. Here, it is worth mentioning that the dangling pendant poly-sulfidic crosslink precursor may also get converted into the most stable mono-sulfidic crosslink precursor during the desulfuration process. Therefore, the network of NR-S being formed just before its reversion at 180 °C (or 190 °C), as shown in Fig. 8b, will be modified after the reversion phase, as shown in Fig. 8c. It is clear from the figure that the restructured

network comprises a mixture of mono- and di-sulfidic crosslinks, cyclic sulfides, accelerator-terminated mono-sulfidic crosslink precursors, conjugated diene and triene-diffused NR chains, and some NR chains with unreacted double bonds. If heating is maintained at this stage, the accelerator-terminated mono-sulfidic crosslink precursors which were trapped within the initially framed network may produce additional mono-sulfidic crosslinks by interacting with the unreacted unsaturated NR chains. As a result, after 60 min of curing, the network structure of NR-S will resemble that in Fig. 8d. This newly formed mono-sulfidic crosslink might be one of the reasons for the post-reversion cure upturn in NR-S at 180 °C or beyond.

Post-reversion Diels–Alder reaction between the rubber chains

As mentioned earlier, a number of studies have claimed that reversion in the NR/CV system leads to the creation of some amount of conjugated double bonds on the NR backbone [19–21]. It is well known that the conjugated double bonds can undergo the Diels–Alder reaction if there are any dienophiles (compounds having active diene units) in the system [27]. Therefore, to tap the conjugated diene-modified NR being generated (Fig. 8c) during the reversion phase of NR-S, 1 phr of a dienophile known as perkalink 900 was introduced into the recipe (NR-SPL1). Represented in Fig. 9 is the curing curve of NR-SPL1 at 180 °C for 1 h. For a comparative evaluation, the curing curve of NR-S at 180 °C for 1 h is also included in the same figure. Both NR-S and NR-SPL1 exhibited a similar curing profile until 2.5 min of

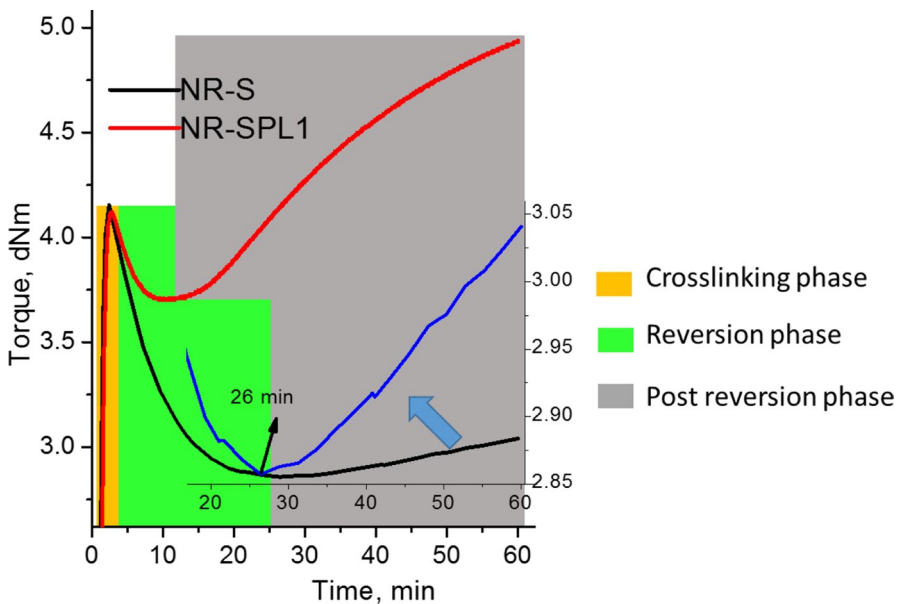


Fig. 9 Curing curves of NR-S and NR-SPL1 at 180 °C, 1 h. (The inset curve is the enlarged view of NR-S from 26 to 60 min of curing)

curing. However, after a sharp reversion from 2.5 to 12 min, NR-SPL1 exhibited an upturn curing behavior with a 33.76% increase in rheometric torque after 60 min of curing. One of the promising reasons for this cure upturn is attributed to the Diels–Alder reaction between the conjugated diene-diffused NR chains being generated at the point of reversion and the maleimide moieties of PL, as shown in Fig. 10a, b [28, 29]. Here, Fig. 10a demonstrates the network generated during the reversion phase (2.5–12 min). As can be seen, PL remained inactive within the network till the end of the reversion phase (up to 12 min). However, as heating continues, it becomes part of the network via the Diels–Alder reaction (as shown in Fig. 10b) and makes the resultant network strong enough to prevent any further reversion. The physical manifestation of this Diels–Alder reaction was the sharp upturn of the curing curve immediately after the reversion. Here it is worth mentioning that the post-reversion Diels–Alder reaction between the conjugated diene-modified NR and PL seems to be faster. Hence, if PL is present in the system, there will be very little chance for post-reversion mono-sulfidic crosslink production between the rubber-bound mono-sulfidic crosslink precursor and the unsaturated NR chains.

On the other hand, the reversion in NR-S continued from 2.5 to 26 min. From there, it exhibited an upturn behavior with a 7% increase in rheometric torque until 60 min of curing. To get a clear picture of this upturn cure behavior, an enlarged view of the NR-S curve from 26 to 60 min in blue color is represented as an inset in Fig. 9. The torque continued to increase by 16.2% as we extended the curing time to 2 h (see Fig. 6a). Since there is no dieneophile (like PL) present in NR-S, this post-reversion cure upturn is probably due to the results of two chemical reactions or modifications within the broken network of NR-S. One potential cause could be the formation of post-reversion mono-sulfidic crosslinks, as illustrated in Fig. 8b–d. The other possibility could be the inter-chain Diels–Alder reaction between the unsaturated portion of NR that was left untouched during the sulfur curing phase and the in-situ-formed conjugated diene on the NR backbone, as shown in Fig. 11a,

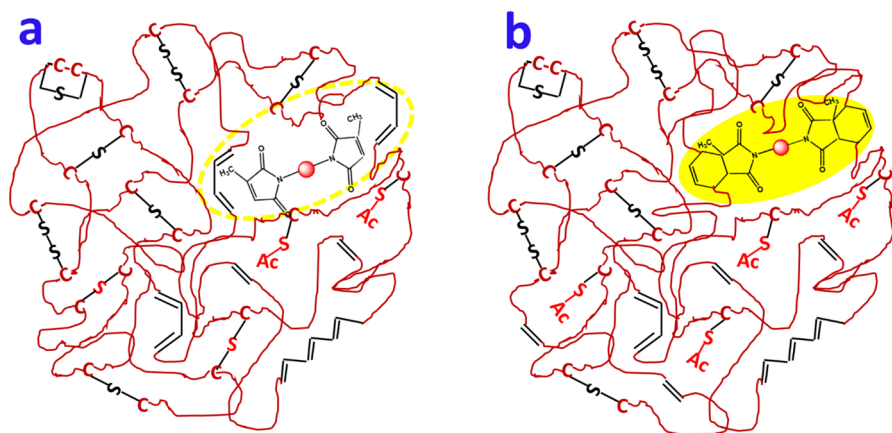


Fig. 10 Presumed network states in NR-SPL1 at 180 °C under different curing time **a** up to 12 min of curing **b** after 60 min of curing

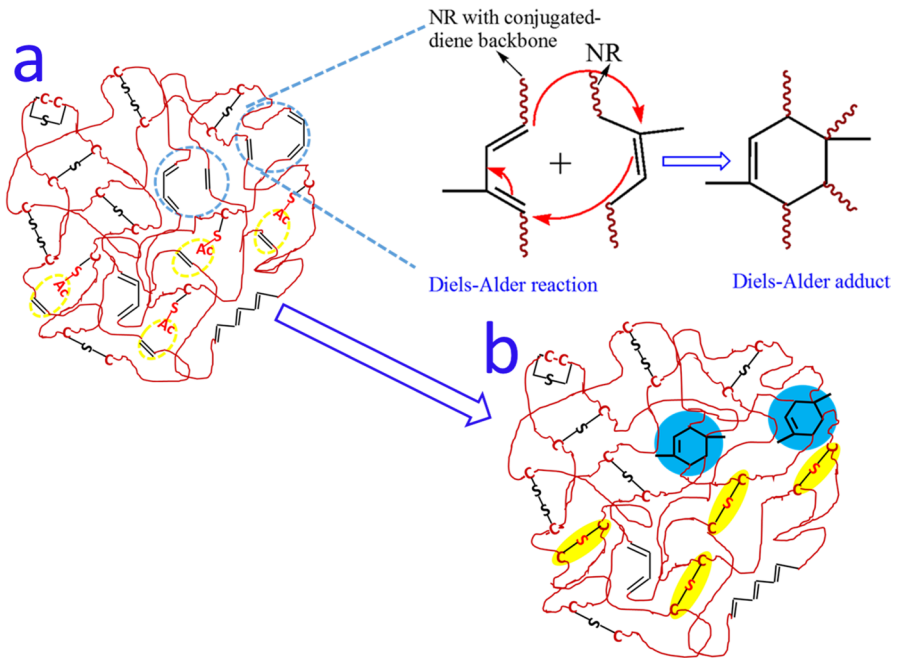


Fig. 11 Presumed network state of NR-S **a** up to 26 min of curing at 180 °C **b** after 60 min of curing at 180 °C due to post-reversion Diels–Alder reaction

b. Here, it has to be remembered that this reaction is believed to take place between a macro-diene (conjugated diene-modified NR) and a macro-dienophile (unsaturated NR) within the partially broken network. Therefore, the magnitude of torque due to this reaction might be relatively low when compared to the DA reaction between the conjugated NR and the low-molecular-weight PL. The lower activity of NR as a dienophile (because of the electron-donating methyl group attached to the unsaturated carbon atom) might be another reason for the low magnitude of the post-reversion crosslinking torque due to this reaction.

Conclusions

This investigation describes the post-reversion upturn of natural rubber with a conventional accelerator sulfur system at a higher curing temperature. One of the primary reasons for the post-reversion upturn was identified as the reconstruction of the network that was damaged during the reversion phase. By evaluating the chemical crosslink densities of the samples prepared under different curing time and temperature, it has been presumed that certain crosslinking reactions are responsible for the post-reversion network rebuilding. The RPA cure-strain sweep analysis based on the shear storage modulus of the network formed during the curing, reversion, and post-reversion phases provided additional proof for the possibility of crosslinking reactions in the post-reversion phase. Based on the knowledge conceived from the

previous literature and also from the meticulous analysis of our own experimental results, two possibilities have been proposed to interpret the post-reversion upturn of the curing curve. One of the suggested mechanisms describes the possibilities of the formation of post-reversion mono-sulfidic crosslinks by the action of mono-sulfidic crosslink precursors that were left unreacted within the broken network with the allylic carbons of the NR chains. The second possibility is considered to be the post-reversion inter-chain Diels–Alder reaction between the conjugated diene-diffused natural rubber and the unmodified unsaturated moieties of natural rubber. This probability was experimentally supported by confirming the Diels–Alder reaction between the in-situ formed diene-modified NR chains at the point of reversion and a low-molecular-weight dienophile known as 1, 3-bis (citraconimidomethyl) benzene.

Acknowledgements This work was supported by the Ministry of Education, Youth and Sports of the Czech Republic—DKRVO (RP/CPS/2022/006).

Author contributions Marek Poschl done material preparation and data collection. Shibulal Gopi Sathi contributed to conceptualization and writing-original draft preparation. Shibulal Gopi Sathi and Marek Poschl helped in methodology, formal analysis, and investigation. Shibulal Gopi Sathi and Radek Stocек helped in writing-review and editing and supervision. Radek Stocек done funding acquisition and resources.

Funding Open access publishing supported by the National Technical Library in Prague. This study was funded by Ministry of Education, Youth and Sports of the Czech Republic, DKRVO(RP/CPS/2022/006), DKRVO(RP/CPS/2022/006), DKRVO(RP/CPS/2022/006).

Data availability No datasets were generated or analysed during the current study.

Declarations

Conflict of interest The authors declare no competing interests.

Open Access This article is licensed under a Creative Commons Attribution 4.0 International License, which permits use, sharing, adaptation, distribution and reproduction in any medium or format, as long as you give appropriate credit to the original author(s) and the source, provide a link to the Creative Commons licence, and indicate if changes were made. The images or other third party material in this article are included in the article's Creative Commons licence, unless indicated otherwise in a credit line to the material. If material is not included in the article's Creative Commons licence and your intended use is not permitted by statutory regulation or exceeds the permitted use, you will need to obtain permission directly from the copyright holder. To view a copy of this licence, visit <http://creativecommons.org/licenses/by/4.0/>.

References

1. Akiba M, Hashim AS (1997) Vulcanization and crosslinking in elastomers. *Prog Polym Sci* 22:475–521. [https://doi.org/10.1016/S0079-6700\(96\)00015-9](https://doi.org/10.1016/S0079-6700(96)00015-9)
2. Kruželák J, Sýkora R, Hudec I (2016) Sulphur and peroxide vulcanisation of rubber compounds-overview. *Chem Pap* 70:1533–1555. <https://doi.org/10.1515/chempap-2016-0093>
3. Rajesh BR, Shibulal GS, Chandra AK, Naskar K (2013) Compounding and vulcanization. In: Visakh P, Thomas S, Chandra AK, Mathew A (ed) *Advances in elastomers I. Blends and interpenetrating networks*. Springer, Berlin, Heidelberg, pp 83–138
4. Coran AY (2003) Chemistry of the vulcanization and protection of elastomers: a review of the achievements. *J Appl Polym Sci* 87:24–30. <https://doi.org/10.1002/app.11659>
5. Saville B, Watson AA (1967) Structural characterization of sulfur-vulcanized rubber networks. *Rubber Chem Technol* 40:100–148. <https://doi.org/10.5254/1.3539039>

6. Dick JS, Henry P, Erwin S (1995) Alternate instrumental methods of measuring scorch and cure characteristic. *Polym Test* 14:45–84. [https://doi.org/10.1016/0142-9418\(95\)90615-N](https://doi.org/10.1016/0142-9418(95)90615-N)
7. Dick JS, Henry P (1996) Applications for the curemeter maximum cure rate in rubber compound development process control and cure kinetic studies. *Polym Test* 15:207–243. [https://doi.org/10.1016/0142-9418\(95\)00033-X](https://doi.org/10.1016/0142-9418(95)00033-X)
8. Morrison NJ, Porter M (1984) Temperature effects on the stability of intermediates and crosslinks in sulfur vulcanization. *Rubber Chem Technol* 57:63–85. <https://doi.org/10.5254/1.3536002>
9. Kanoktip B, Chudej D, Kanyarat B (2016) Effect of sulfur to accelerator ratio on crosslink structure, reversion, and strength in natural rubber. *Rubber Chem Technol* 450–464. <https://doi.org/10.5254/rct.16.85963>
10. Milani G, Leroy E, Milani F, Deterre R (2013) Mechanistic modeling of reversion phenomenon in sulphur cured natural rubber vulcanization kinetics. *Polym Test* 32:1052–1063. <https://doi.org/10.1016/j.polymertesting.2013.06.002>
11. Sathi SG, Stoček R, Kratina O (2020) Reversion free high-temperature vulcanization of cis-polybutadiene rubber with the accelerated-sulfur system. *EXPRESS Polym Lett*. 14:823–837. <https://doi.org/10.3144/expresspolymlett.2020.68>
12. Flory PJ, Rehner J (1943) Statistical mechanics of crosslinked polymer networks I. Rubberlike elasticity. *J Chem Phys* 11:512–520. <https://doi.org/10.1063/1.1723791>
13. Flory PJ, Rehner J (1943) Statistical mechanics of crosslinked polymer networks II. Swelling. *J Chem Phys* 11:521–526. <https://doi.org/10.1063/1.1723792>
14. Kim DY, Park JW, Lee DY, Seo KH (2020) Correlation between the crosslink characteristics and mechanical properties of natural rubber compound via accelerators and reinforcement. *Polymers* 12:2020–2023. <https://doi.org/10.3390/polym12092020>
15. Kumar NR, Chandra AK, Mukhopadhyay R (1997) Effect of 1,3-bis(citraconimidomethyl) benzene on the aerobic and anaerobic ageing of diene rubber vulcanizates. *J Mater Sci* 32:3717–3725. <https://doi.org/10.1023/A:1018655102644>
16. Davis LH, Sullivan AB, Coran AY (1987) New curing system components. *Rubber Chem Technol* 60:125–139. <https://doi.org/10.5254/1.3536113>
17. Prasenjeet G, Santhoji K, Priyan P, James MC, Venkat V (2003) Sulfur vulcanization of natural rubber for benzothiazole accelerated formulations: from reaction mechanisms to a rational kinetic model. *Rubber Chem Technol* 76:592–693. <https://doi.org/10.5254/1.3547762>
18. Santhosh AA, Kuruvilla J, Sabu T (2005) Recent developments in crosslinking of elastomers. *Rubber Chem Technol* 78:458–488. <https://doi.org/10.5254/1.3547892>
19. Frederic JL, Edwin JP, James ES (1964) Some changes in double-bond structure during the vulcanization of natural rubber. *J Res Natl Bur Stand A Phys Chem*. 68A:499–511. <https://doi.org/10.6028/jres.068A.047>
20. Bornstein D, Pazur RJ (2020) The sulfur reversion process in natural rubber in terms of crosslink density and crosslink density distribution. *Polym Test* 88:106524. <https://doi.org/10.1016/j.polymertesting.2020.106524>
21. Bandzierz KS, Reuvekamp LAEM, Dryzek J, Dierkes WK, Blume A, Bieliński DM (2019) Effect of polymer chain modifications on elastomer properties. *Rubber Chem Technol* 92:69–89. <https://doi.org/10.5254/RCT.18.82685>
22. Morrison NJ, Porter M (1984) Temperature effects on the stability of intermediates and crosslinks in sulfur vulcanization. *Rubber Chem Technol* 57:63–85. <https://doi.org/10.5254/1.3536002>
23. Patrick JH, Kevin DOJ (1994) Applications of Raman spectroscopy to the analysis of natural rubber. *Spectrochim Acta Part A: Mol Spectrosc* 50:1987–1997. [https://doi.org/10.1016/0584-8539\(94\)80210-6](https://doi.org/10.1016/0584-8539(94)80210-6)
24. Datta RN, Hofstraat JW, Geurts FAJ, Talma AG (1999) Fourier transform Raman spectroscopy for characterization of natural rubber reversion and of antireversion agents. *Rubber Chem Technol* 72:829–843. <https://doi.org/10.5254/1.3538835>
25. Zaper AM, Koenig JL (1987) Solid state carbon-13 NMR studies of vulcanized elastomers. II, sulfur vulcanization of natural rubber. *Rubber Chem Technol*. 60:252–277. <https://doi.org/10.5254/1.3536129>
26. Loo CT (1974) High temperature vulcanization of elastomers: 2. Network structures in conventional sulphenamide-sulphur natural rubber vulcanizates. *Polymer* 15:357–365. [https://doi.org/10.1016/0032-3861\(74\)90177-3](https://doi.org/10.1016/0032-3861(74)90177-3)
27. Gheneim R, Perez-Berumen C, Gandini A (2002) DielsAlder reactions with novel polymeric dienes and dienophiles: synthesis of reversibly cross-linked elastomers. *Macromol* 35:7246–7253. <https://doi.org/10.1021/ma020343c>

28. Sathi SG, Harea E, Machů A, Stoček R (2021) Facilitating high-temperature curing of natural rubber with a conventional accelerated-sulfur system using a synergistic combination of bismaleimides. *eXPRESS Polym Lett.* 15:16–27. <https://doi.org/10.3144/expresspolymlett.2021.3>
29. Sathi SG, Jeon J, Won J, Nah C (2018) Enhancing the efficiency of zinc oxide vulcanization in brominated poly (isobutylene-co-isoprene) rubber using structurally different bismaleimides. *J Polym Res* 25:108–121. <https://doi.org/10.1007/s10965-018-1512-8>

Publisher's Note Springer Nature remains neutral with regard to jurisdictional claims in published maps and institutional affiliations.